Mon. Not. R. Astron. Soc. **000**, 1–6 (2005) Printed 3 December 2004 (MN LaTeX style file v2.2)

Saturation of the Magnetorotational Instability

E. Knobloch[1,2]⋆ and K. Julien[3]
[1] *Department of Applied Mathematics, University of Leeds, Leeds LS2 9JT, UK*
[2] *Department of Physics, University of California, Berkeley, CA 94720, USA*
[3] *Department of Applied Mathematics, University of Colorado, Boulder, CO 80309, USA*

Accepted 200* December **. Received 200* December **; in original form 2004 December **

ABSTRACT
An analytical theory is developed that describes asymptotically exactly the process of nonlinear saturation of the magnetorotational instability. The theory employs the shearing sheet approximation with arbitrary (but linear) shear flow. The theory shows that the instability saturates by extracting energy from the shear, and modifying the shear responsible for it. The saturation process requires both viscous and ohmic dissipation. The theory also describes the approach from small amplitude perturbations to the final strongly nonlinear saturated state.

Key words: accretion disks – magnetorotational instability.

1 INTRODUCTION

Accretion is a process of fundamental importance in astrophysics. However, accretion can only occur in the presence of an efficient mechanism for angular momentum extraction. Over the years many processes have been suggested that might lead to efficient accretion (Balbus & Hawley (1998)). In general, hydrodynamical instabilities, be they shear instabilities (in radial or vertical directions Dubrulle et al. (2004)) or baroclinic instabilities (Knobloch & Spruit (1986)) are insufficient. So are spiral shock waves resulting from acoustic perturbations (Rózyczka & Spruit (1992)), or global modes involving over-reflection of negative energy waves between the inner edge of the disk and the corotation radius (Papaloizou & Pringle (1992)). Other authors have considered convective disks (Ryu & Goodman (1992); Balbus et al. (1996); Stone & Balbus (1996)). In 1991 Balbus and Hawley (Balbus & Hawley (1991); Hawley & Balbus (1991)) pointed out that a classical instability (Velikhov (1959); Chandrasekhar (1960)), since called the magnetorotational instability (or MRI, for short), is particularly effective in this respect. This instability relies on the presence of a weak poloidal field and occurs in hot disks whenever the angular velocity Ω in the disk decreases outward ($d\Omega/dr < 0$). The instability grows by extracting energy from the resulting shear. Particularly noteworthy is the fact that the instability occurs on a dynamic time scale, $\tau_{MRI} \sim \Omega^{-1}$ and that it is fundamentally axisymmetric. The instability has a small wavelength in the direction parallel to the rotation and magnetic field and takes the form of thin sheets of matter moving alternately radially inwards and outwards. It is known that sufficient dissipation stabilizes this instability (Acheson & Hide (1973)) but in accretion disks dissipative processes are weak and the instability is unhindered by such processes (Balbus & Hawley (1991, 1998)). It is not true, however, that dissipation is always negligible. Indeed, as shown in the present paper, for the saturation of the instability, small dissipation, both viscous and ohmic, is required.

It is believed by some that the MRI instability saturates by generating turbulence which in turn enhances turbulent dissipation, thereby quenching the instability back to threshold. This type of idea is common in astrophysics, and may indeed apply in some circumstances. However, it must be recognized that this idea is essentially a linear one, and that it cannot modify the angular velocity distribution that feeds the instability. In the present paper we adopt a different perspective, and show, using an asymptotically exact procedure, that the MRI does modify the angular velocity distribution as it grows, and that it may, in some cases, continue until solid body rotation is established.

The method used in the present paper has its origins in the work of Blennerhassett & Bassom (1994) on the theory of Görtler vortices and related problems. Subsequently it has been used with considerable effect to study rapidly rotating convection in both two (Bassom & Zhang (1994); Julien & Knobloch (1997, 1998)) and three dimensions (Julien et al. (1998); Julien & Knobloch (1999)), as well as convection in a strong magnetic field (Matthews (1999); Julien et al. (1999, 2000)). The method takes advantage of the small scale of the instability which is used as an expansion parameter. The method is thus ideally suited for fingering instabilities such as the MRI. In the following we show that it can be applied in a straightforward fashion to the MRI in the astrophysically interesting regime in which rotation and shear dominate the effects of the (poloidal) magnetic field, which

⋆ E-mail: knobloch@px1.berkeley.edu (EK); julien@colorado.edu (KJ)

is in turn more important than viscous and ohmic dissipation. Despite this both dissipative processes determine the final equilibrium state. The present theory is thus ideally suited for comparison with numerical simulations, such as that of Kersalé et al. (2004), in which the dissipative scales are fully resolved.

The paper is organized as follows. In Section 2 we describe the shearing sheet formulation of the problem, and introduce the scalings used to characterize the fully nonlinear equilibrated state. We then proceed to compute in detail the properties of this state. Section 3 describes the evolution of small random perturbations towards this final state, indicating that the final state is stable. The paper concludes with a brief conclusion.

2 THE SHEARING SHEET APPROXIMATION

In the local approximation we may suppose that the azimuthal shear is locally linear, $\mathbf{U_0} = (0, \sigma x, 0)$, $\sigma < 0$, and that a constant magnetic field $\mathbf{B_0} = (0, B_{tor}, B_{pol})$ is present. Here (x, y, z) are local Cartesian coordinates with x pointing in the radial direction, y in the azimuthal direction and z parallel to the rotation axis. Axisymmetric perturbations $(u, v, w) = (-\psi_z, v, \psi_x)$ and $(a, b, c) = B_{pol}(-\phi_z, b, \phi_x)$ of this state satisfy the equations

$$\nabla^2\psi_t + 2\Omega v_z + J(\psi, \nabla^2\psi) = v_A^2\nabla^2\phi_z + v_A^2 J(\phi, \nabla^2\phi) + \nu\nabla^4\psi, \tag{1}$$

$$v_t - (2\Omega + \sigma)\psi_z + J(\psi, v) = v_A^2 b_z + v_A^2 J(\phi, b) + \nu\nabla^2 v, \tag{2}$$

$$\phi_t + J(\psi, \phi) = \psi_z + \eta\nabla^2\phi, \tag{3}$$

$$b_t + J(\psi, b) = v_z - \sigma\phi_z + J(\phi, v) + \eta\nabla^2 b, \tag{4}$$

where $v_A^2 \equiv B_{pol}^2/\mu_0\rho U^{*2}$ is proportional to the Alfvén speed associated with the poloidal or vertical magnetic field, $J(f, g) = f_x g_z - f_z g_x$, and Ω, ν η represent the dimensionless rotation rate, kinematic viscosity and ohmic diffusivity, nondimensionalized using a velocity scale U^* and a length scale L^*. Note that B_{tor} drops out of these equations. This is a consequence of the local approximation which leads to the suppression of hoop stresses (Knobloch (1996)). However, the azimuthal field perturbation b will prove to be important in what follows. The local approximation also implies that the MRI is an exponentially growing instability; this is not necessarily the case in polar coordinates with nonzero toroidal field (Knobloch (1992)).

In the following we assume that the MRI takes the form of thin fingers propagating in the x direction, as indicated by linear stability theory (Balbus & Hawley (1991)) and subsequent numerical experiments (Hawley & Balbus (1991, 1992)). By definition, such fingers have a small transverse width. Accordingly, in the following we introduce a small parameter $\epsilon \ll 1$ and suppose that all derivatives in the z direction are large, i.e., we scale z such that in the new variable ∂_z is replaced by $\epsilon^{-1}\partial_z$. In addition we suppose that in an appropriate dimensionless sense the dissipative processes are small, and let $(\nu, \eta) = \epsilon(\hat\nu, \hat\mu)$. At the same time we assume that the disk is rotating rapidly and that the dimensionless shear rate is also large, i.e., we set $(\Omega, \sigma) = \epsilon^{-1}(\hat\Omega, \hat\sigma)$ while keeping the Alfvén speed of order unity. These assumptions reflect the conditions generally believed to be present in accretion disks: the shear is the dominant source of energy for the instability, but the instability itself requires the presence of a (weaker) vertical magnetic field. Dissipative effects are weaker still but cannot be ignored since they are ultimately responsible for the saturation of the instability.

In parallel with the above assumptions about physical conditions in the disk we need to make further assumptions about the relative magnitude of the various fields. We find that the assumption $(\psi, \phi) \to \epsilon(\psi, \phi)$, $(v, b) \to \epsilon^{-1}(v, b)$. leads to a self-consistent fully nonlinear stationary solution, satisfying the scaled equations

$$2\epsilon^{-3}\hat\Omega v_z + \epsilon J(\psi, \partial_x^2 + \epsilon^{-2}\partial_z^2)\psi) = v_A^2(\partial_x^2 + \epsilon^{-2}\partial_z^2)\phi_z + \epsilon v_A^2 J(\phi, (\partial_x^2 + \epsilon^{-2}\partial_z^2)\phi) + \epsilon^2\hat\nu(\partial_x^2 + \epsilon^{-2}\partial_z^2)^2\psi, \tag{5}$$

$$-\epsilon^{-1}(2\hat\Omega + \hat\sigma)\psi_z + \epsilon^{-1}J(\psi, v) = \epsilon^{-2}v_A^2 b_z + \epsilon^{-1}v_A^2 J(\phi, b) + \hat\nu(\partial_x^2 + \epsilon^{-2}\partial_z^2)v, \tag{6}$$

$$\epsilon J(\psi, \phi) = \psi_z + \epsilon^2\hat\eta(\partial_x^2 + \epsilon^{-2}\partial_z^2)\phi, \tag{7}$$

$$\epsilon^{-1}J(\psi, b) = \epsilon^{-2}v_z - \epsilon^{-1}\hat\sigma\phi_z + \epsilon^{-1}J(\phi, v) + \hat\eta(\partial_x^2 + \epsilon^{-2}\partial_z^2)b. \tag{8}$$

To solve these equations we posit an expansion of the form $\psi(x, z) = \psi_0(x, z) + \epsilon\psi_1(x, z) + \ldots$ with similar expressions for the other three fields, and look for structures that are periodic in the z direction. From Eqs. (6), (8) it now follows that at $O(\epsilon^{-2})$

$$v_A^2 b_{0z} + \hat\nu v_{0zz} = 0, \qquad v_{0z} + \hat\eta b_{0zz} = 0, \tag{9}$$

and hence that

$$v_0 = V(x), \qquad b_0 = B(x), \tag{10}$$

while from Eq. (7) we obtain at $O(1)$

$$\psi_0 + \hat\eta\phi_{0z} = 0. \tag{11}$$

At next order we obtain the following three equations:

$$-(2\hat\Omega + \hat\sigma)\psi_{0z} + J(\psi_0, v_0) = v_A^2 b_{1z} + v_A^2 J(\phi_0, b_0) + \hat\nu v_{1zz}, \tag{12}$$

$$0 = \psi_{0z} + \hat\eta\phi_{0zz}, \tag{13}$$

$$J(\psi_0, b_0) = v_{1z} - \hat\sigma\phi_{0z} + J(\phi_0, v_0) + \hat\eta b_{1zz}. \tag{14}$$

In the following we write

$$\psi_0 = \frac{1}{2}(\Psi(x)\, e^{inz} + \text{c.c.}), \quad v_1 = \frac{1}{2}(\mathcal{V}(x)\, e^{inz} + \text{c.c.}), \tag{15}$$
$$\phi_0 = \frac{1}{2}(\mathcal{F}(x)\, e^{inz} + \text{c.c.}), \quad b_1 = \frac{1}{2}(\mathcal{B}(x)\, e^{inz} + \text{c.c.}).$$

From equations (12-14) it now follows that

$$\mathcal{V} = \frac{(v_A^2 + \hat\eta^2 n^2)V' + \hat\eta^2 n^2(2\hat\Omega + \hat\sigma) + v_A^2\hat\sigma}{n\hat\eta(v_A^2 + \hat\nu\hat\eta n^2)}\, i\Psi, \tag{16}$$

$$\mathcal{F} = \frac{i\Psi}{\hat\eta n}, \tag{17}$$

$$\mathcal{B} = \frac{i(v_A^2 + \hat{\nu}\hat{\eta}n^2)B' + n(\hat{\nu}(\hat{\sigma} + V') - \hat{\eta}(2\hat{\Omega} + \hat{\sigma} + V'))}{n\hat{\eta}(v_A^2 + \hat{\nu}\hat{\eta}n^2)}\Psi. \quad (18)$$

Finally, Eqs. (6), (8) yield at $O(1)$ the results

$$-(2\hat{\Omega} + \hat{\sigma})\psi_{1z} + J(\psi_0, v_1) + J(\psi_1, v_0) = v_A^2 b_{2z} + v_A^2 J(\phi_0, b_1) + v_A^2 J(\phi_1, b_0) + \hat{\nu}(v_{0xx} + v_{2zz}), \quad (19)$$

and

$$J(\psi_0, b_1) + J(\psi_1, b_0) = v_{2z} - \hat{\sigma}\phi_{1z} + J(\phi_0, v_1) + J(\phi_1, v_0) + \hat{\eta}(b_{0xx} + b_{2zz}). \quad (20)$$

Averaging these equations over z and using the fact that the quantities $\psi_0, \psi_1, v_1, v_2, \phi_0, \phi_1, b_1, b_2$ are all, by construction, periodic in z with zero mean yields the following pair of equations:

$$\hat{\nu}V'' = \partial_x(\overline{\psi_0 v_{1z}}) - v_A^2 \partial_x(\overline{\phi_0 b_{1z}}), \quad (21)$$

$$\hat{\eta}B'' = \partial_x(\overline{\psi_0 b_{1z}}) - \partial_x(\overline{\phi_0 v_{1z}}). \quad (22)$$

In the absence of boundaries in the x direction we must assume that V' and B' are *constant* across any domain in x, and satisfy

$$\hat{\nu}V' = \overline{\psi_0 v_{1z}} - v_A^2 \overline{\phi_0 b_{1z}}, \quad (23)$$

$$\hat{\eta}B' = \overline{\psi_0 b_{1z}} - \overline{\phi_0 v_{1z}}. \quad (24)$$

Evaluating the averages in terms of Ψ and solving for V' and B' now yields

$$V'(x) = -\frac{\frac{1}{2}\beta|\Psi|^2}{\hat{\nu} + \frac{1}{2}\alpha|\Psi|^2}, \quad (25)$$

$$B'(x) = 0, \quad (26)$$

where

$$\alpha = \frac{\hat{\nu}v_A^2 + \hat{\eta}^3 n^2}{\hat{\eta}^2(v_A^2 + \hat{\nu}\hat{\eta}n^2)}, \quad (27)$$

$$\beta = \frac{(2\hat{\Omega} + \hat{\sigma})\hat{\eta}^3 n^2 + v_A^2(\hat{\sigma}\hat{\nu} - 2\hat{\Omega}\hat{\eta})}{\hat{\eta}^2(v_A^2 + \hat{\nu}\hat{\eta}n^2)}. \quad (28)$$

Equation (25) determines the equilibrated shear V' in terms of the streamfunction amplitude $|\Psi|$ and wavenumber n of the instability. As we show next we can obtain an additional relation between $|\Psi|$ and n from the ψ equation (5).

This equation yields at leading order

$$2\hat{\Omega}v_{1z} = v_A^2 \phi_{0zzz} + \hat{\nu}\psi_{0zzzz}, \quad (29)$$

or, equivalently,

$$2\hat{\Omega}[(v_A^2 + \hat{\eta}^2 n^2)V' + (2\hat{\Omega} + \hat{\sigma})\hat{\eta}^2 n^2 + \hat{\sigma}v_A^2] + n^2(v_A^2 + \hat{\nu}\hat{\eta}n^2)^2 = 0. \quad (30)$$

Except for the presence of the additional shear rate V' this is nothing but the dispersion relation for the MRI in our scaling regime; we refer to (30) as the *nonlinear* dispersion relation. For each wavenumber n this relation determines the equilibrium shear V' and through equation (25) the corresponding streamfunction amplitude Ψ. One finds

$$\tfrac{1}{2}|\Psi|^2\left[4\hat{\Omega}^2 v_A^2 \hat{\eta} + n^2\left(v_A^2 + \hat{\nu}\hat{\eta}n^2\right)\left(\hat{\nu}v_A^2 + \hat{\eta}^3 n^2\right)\right] + \hat{\nu}\hat{\eta}^2 n^2(v_A^2 + \hat{\nu}\hat{\eta}n^2)^2 + 2\hat{\Omega}\hat{\sigma}\hat{\nu}\hat{\eta}^2 v_A^2 + 2\hat{\Omega}(2\hat{\Omega} + \hat{\sigma})\hat{\nu}\hat{\eta}^4 n^2 = 0. \quad (31)$$

Note that this equation *requires* that $\hat{\sigma} < 0$.

Equation (31) determines the amplitude $|\Psi|$ as a function of the imposed shear rate $\hat{\sigma}$ for each choice of wavenumber n, and therefore represents the *bifurcation equation* for this problem. This relation has one particularly interesting limit: if we suppose that the (scaled) rotation dominates the (scaled) magnetic field which in turn dominates the (scaled) dissipation, Eq. (31) reduces to

$$|\Psi|^2 = -\frac{\hat{\sigma}}{\hat{\Omega}}\hat{\nu}\hat{\eta}, \quad (32)$$

providing a simple relation between the imposed shear rate $\hat{\sigma}$ and the resulting equilibrated amplitude $|\Psi|$, and one that is *independent* of the (scaled) wavenumber n. Thus the (unscaled) radial speed of the MRI fingers is given by

$$u \sim n|\Psi| = n\left(-\frac{\hat{\sigma}}{\hat{\Omega}}\right)^{1/2}(\hat{\nu}\hat{\eta})^{1/2}, \quad (33)$$

a speed that is of the order of the Alfvén speed v_A. Note that this speed is the geometric mean between the energy-containing shear flow $\sigma' L^*$ and the dissipative scale velocities ν/L^* or η/L^*, and is accompanied by much slower $O(\epsilon)$ motions in the vertical. More significantly, equation (25) shows that the corresponding equilibrated shear $V' = -\hat{\sigma}$! It follows that in this regime the MRI continues until it extracts all the energy from the imposed shear and uniform rotation results, a conclusion supported by the original simulations of the MRI by Hawley & Balbus (1991). Indeed, these authors also point to the important role played by reconnection in providing a saturation mechanism, a process that appears explicitly, via the diffusivity η, in the prediction (33).

The theory thus far remains unsatisfactory in one respect: the wavenumber n is not specified. It is usual in these circumstances to use the wavenumber n_{max} of the fastest growing mode. According to linear theory the growth rate λ is given by

$$2\hat{\Omega}[(2\hat{\Omega}+\hat{\sigma})(\lambda+\hat{\eta}n^2)^2+\hat{\sigma}v_A^2 n^2]+[(\lambda+\hat{\nu}n^2)(\lambda+\hat{\eta}n^2)+v_A^2 n^2]^2 = 0, \quad (34)$$

and n_{max} is defined by $d\lambda/dn = 0$. In Figs. 1-3 we show the result of using this wavenumber to compute the saturated state shear V'_{max} and the associated streamfunction amplitude $|\Psi|_{max}$. As already indicated this choice of n does not affect certain regimes, and in particular the astrophysically relevant regime (32). Figure 1 shows the fastest growing wavenumber n_{max}, the corresponding growth rate λ_{max} and the resulting saturated quantities V'_{max} and $|\Psi|_{max}$ as a function of the ohmic diffusivity η, while Fig. 2 shows these quantities as a function of v_A. Note that V'_{max} is of order one, and saturates after an initial overshoot as η increases, while $|\Psi|_{max}$ increases. This is as expected: resistivity permits the instability to grow to larger amplitude by allowing the magnetic field to move through the accreting material. Figure 2 shows that the saturated value of V'_{max} is substantial even for $0 < v_A \ll 1$, and in fact ultimately drops with increasing v_A. However, the asymptote for large v_A remains finite, indicating that a strong poloidal field does not suppress the instability. Figure 3 shows that the saturated values V'_{max} and $|\Psi|_{max}$ increase approximately linearly with the background shear σ. Note that $n_{max} = 0$ when $V' = -\sigma$, indicating an increase in the vertical wavelength as the MRI approaches

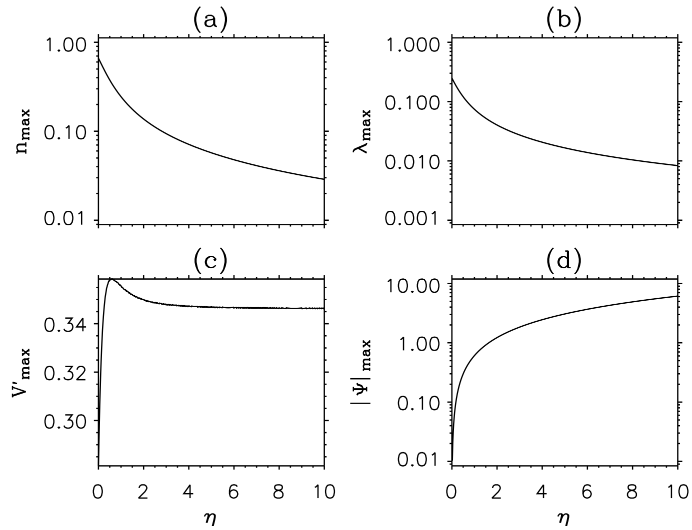

Figure 1. (a) The wavenumber n_{max} of the fastest growing mode, (b) its growth rate λ_{max}, and (c) the resulting shear rate V'_{max} and (d) streamfunction amplitude $|\Psi|_{max}$, as functions of η for $\Omega = 1$, $\sigma = -0.5$, $v_A = 1$, $\nu = \eta$.

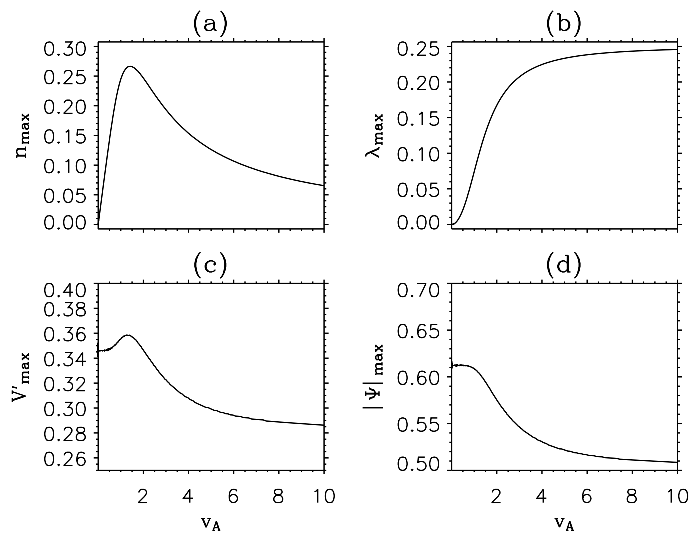

Figure 2. Same as Fig. 1 but as functions of v_A for $\Omega = 1$, $\sigma = -0.5$, $\eta = 1$, $\nu = 1$. The instability is absent when $v_A = 0$.

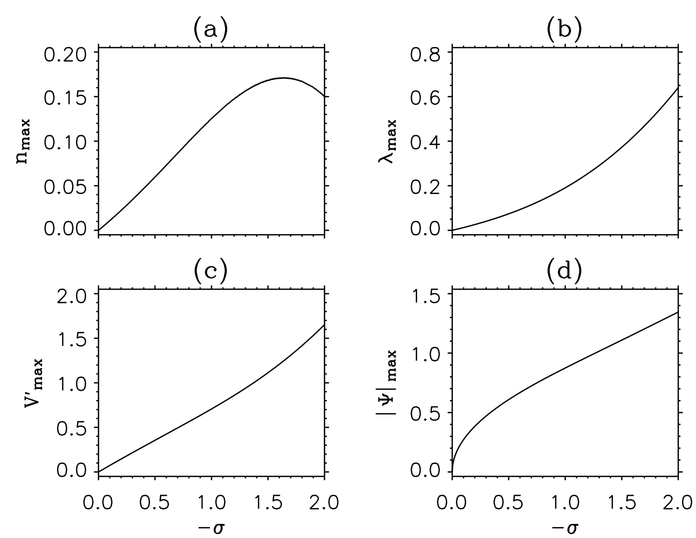

Figure 3. Same as Fig. 1 but as functions of the ambient shear rate σ for $\Omega = 1$, $v_a = 1$, $\eta = 1$, $\nu = 1$. For Kepler shear $\sigma = -0.5$.

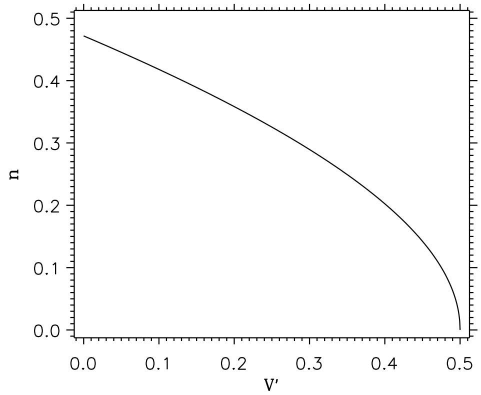

Figure 4. The vertical wavenumber n computed from the nonlinear dispersion relation (30) as a function of V'.

saturation. Figure 4 shows the predicted (scaled) vertical wavenumber n using the nonlinear dispersion relation (30).

3 APPROACH TO THE SATURATED STATE

It is of interest to examine the approach from an initial small amplitude state with $V' \sim 0$ to the final equilibrated state (25). To do this we note that the MRI evolves initially on a dynamical or rotation time scale, i.e., the fast time $\tau \equiv t/\epsilon = O(1)$. However, examining the structure of the equations in the long time limit we also notice that the final approach to the saturated state proceeds on the much slower time scale $T \equiv \epsilon t = O(1)$, i.e., on the resistive time scale. These observations suggest a multiple time scale expansion. It is simpler, however, to assume formally that after a brief ($\tau = O(1)$) transient both V' and B' evolve on a slower time scale than the remaining fields, and take V' and B' to be independent of x. In this regime ψ_0, v_1, ϕ_0 and b_1 are functions of z and τ only, and satisfy

$$v_{1\tau} - (2\hat{\Omega} + \hat{\sigma} + V')\psi_{0z} = v_A^2 b_{1z} - v_A^2 B'\phi_{0z} + \hat{\nu} v_{1zz}, \quad (35)$$

$$\phi_{0\tau} = \psi_{0z} + \hat{\eta}\phi_{0zz}, \quad (36)$$

$$b_{1\tau} - \psi_{0z} B' = v_{1z} - (\hat{\sigma} + V')\phi_{0z} + \hat{\eta} b_{1zz}, \quad (37)$$

together with

$$\psi_{0zz\tau} + 2\hat{\Omega} v_{1z} = v_A^2 \phi_{0zzz} + \hat{\nu}\psi_{0zzzz}. \quad (38)$$

These equations are separable in z and τ. Assuming the Ansatz (15) we obtain

$$\mathcal{V}_\tau + \hat{\nu} n^2 \mathcal{V} = in(2\hat{\Omega} + \hat{\sigma} + V')\Psi + inv_A^2\mathcal{B} - inv_A^2 B'\mathcal{F}, \quad (39)$$

$$\mathcal{F}_\tau + \hat{\eta} n^2 \mathcal{F} = in\Psi, \quad (40)$$

$$\mathcal{B}_\tau + \hat{\eta} n^2 \mathcal{B} = in\Psi B' + in\mathcal{V} - in(\hat{\sigma} + V')\mathcal{F}, \quad (41)$$

$$\Psi_\tau + \hat{\nu} n^2 \Psi - 2in^{-1}\hat{\Omega}\mathcal{V} - inv_A^2\mathcal{F} = 0. \quad (42)$$

Here V' and B' are functions of τ only, and are given by

$$\hat{\nu} V' = -\frac{1}{4} in(\Psi\mathcal{V}^* - \Psi^*\mathcal{V}) + \frac{1}{4} in\, v_A^2(\mathcal{F}\mathcal{B}^* - \mathcal{F}^*\mathcal{B}), \quad (43)$$

$$\hat{\eta} B' = -\frac{1}{4} in(\Psi\mathcal{B}^* - \Psi^*\mathcal{B}) + \frac{1}{4} in(\mathcal{F}\mathcal{V}^* - \mathcal{F}^*\mathcal{V}). \quad (44)$$

These equations capture correctly the saturation process, and in particular the final steady state. The resulting evolution of $V'(\tau)$ and the associated toroidal field gradient $B'(\tau)$ is shown in Fig. 5(a) starting from small amplitude initial conditions. The evolution is shown over times of order τ/ϵ^2 and shows unambiguously the convergence of V' towards its saturated value (25). In contrast B' decays, after some prominent oscillations, to zero, in agreement with (26). For comparison we also show the evolution of the amplitude $|\Psi|$ of the streamfunction (Fig. 5(b)).

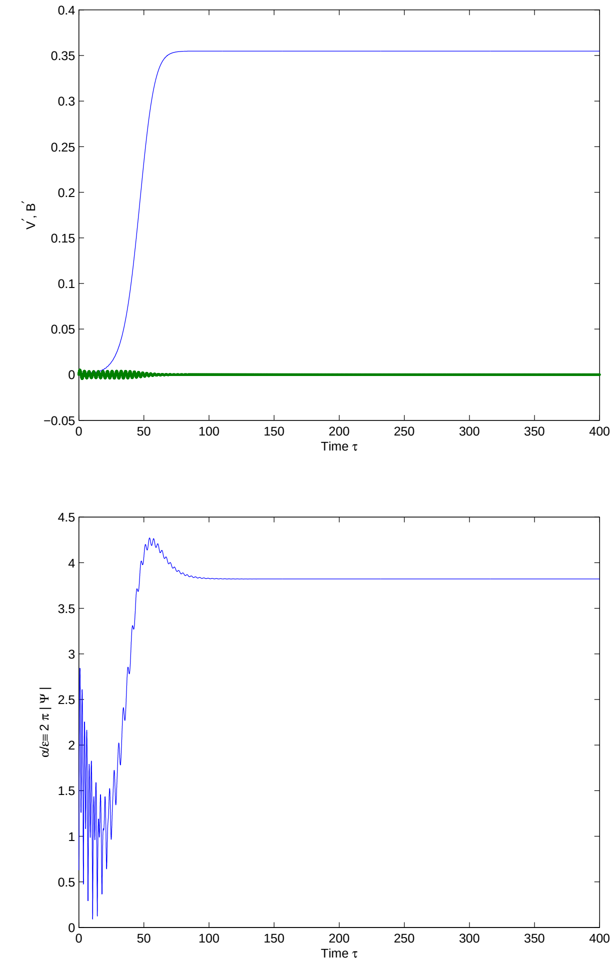

Figure 5. (a) The approach of the MRI to its saturated state, computed for $\Omega = 1$, $\sigma = -0.5$, $v_A = 1$, $\eta = 1$, $\nu = 1$, showing the evolution of V' and B' from small amplitude initial conditions. For these parameter values the equilibrated value $V' = -0.71\sigma$. (b) The corresponding evolution of the Shakura-Sunyaev α parameter, $\alpha \equiv 2\pi\epsilon|\Psi|$.

4 DISCUSSION

In this paper we have shown that a simple scaling suffices to determine and fully characterize a self-consistent equilibrated state of the magnetorotational instability within the shearing sheet approximation. This state is associated with a strong modification of the background instability that feeds the instability, and is ultimately determined by both viscous and ohmic dissipation. In our picture this state is reached after an $O(\Omega^{-1})$ transient followed by a slower evolution on a time scale v_A^{-1}, although the final stages of saturation occur on the much slower time scale η^{-1}, ν^{-1} associated primarily with reconnection. It should be noted that in the theory the equilibrated state consists of laminar axisymmetric 'fingers' and is not a turbulent state such as might result from shear instabilities between neighboring fingers, cf. Goodman & Xu (1994). In some cases, however, the resulting turbulent state may reflect in its statistical properties the presence of the underlying laminar state, cf. Kawahara & Kida (2001), while in others this laminar state *overestimates* the transport properties of the turbulence (Julien et al. (2005)).

It is of interest to compare our results with the shearing sheet simulations of Hawley & Balbus (1991, 1992) and Hawley et al. (1995). Although unable to reach the saturated state these authors also argue that the saturated speed of the fingers should be of order v_A, as predicted by equation (33). However, the prediction (33) shows that while the order of magnitude is correct the saturated speed is not proportional to v_A. Indeed, it is independent of the vertical magnetic field entirely, as might be expected of an instability whose onset is independent of B_z together with a saturation process that relies on efficient reconnection. It is noteworthy that the simulations also indicate a tendency towards solid body rotation as the instability evolves. Finally, the simulations also reveal a tendency towards increasing wavelength as the instability proceeds (Hawley & Balbus (1992)), an observation that is consistent with the predictions of equation (30). Note that the Shakura-Sunyaev (Shakura & Sunyaev (1973)) α parameter, defined by $\alpha = uh$, $h = 2\pi\epsilon/n$, is predicted to be $\alpha = 2\pi\epsilon|\Psi|$ and hence is of order ϵ, see Fig. 5(b).

A significant conclusion of the theory is that numerical simulations of the instability must be able to resolve the dissipative scales in order to determine the equilibrated state correctly. Such computations are currently being performed by a Leeds-Cambridge collaboration (Kersalé et al. (2004)) and a comparison between the theory and simulations will shortly be carried out. Evidently, these simulations must be performed over time scales greater than the ohmic and viscous time scales of the problem. Extension of the theory presented here to include compressibility and circular geometry will be presented in a forthcoming publication.

ACKNOWLEDGMENTS

This work was carried out while the first author (EK) was a participant in a 2004 Newton Institute programme on Magnetohydrodynamics of Stellar Interiors in Cambridge, UK. The second author (KJ) acknowledges financial support from a University of Colorado Faculty Fellowship Award. Both are grateful to S. Tobias for a helpful discussion.

REFERENCES

Acheson, D. & Hide, R., 1973. *Rep. Prog. Phys.*, **36**, 159.
Balbus, S. A. & Hawley, J. F., 1991. *Astrophys. J.*, **376**, 214.
Balbus, S. A. & Hawley, J. F., 1998. *Rev. Mod. Phys.*, **70**, 1.
Balbus, S. A., Hawley, J. F., & Stone, J. M., 1996. *Astrophys. J.*, **467**, 76.
Bassom, A. P. & Zhang, K., 1994. *Geophys. Astrophys. Fluid Dyn.*, **76**, 223.
Blennerhassett, P. J. & Bassom, A. P., 1994. *IMA J. Appl. Maths.*, **52**, 51.
Chandrasekhar, S., 1960. *Proc. Natn. Acad. Sci. USA*, **46**, 53.
Dubrulle, B., Marié, L., Normand, Ch., Richard, D., Hersant, F. & Zahn, J.-P., 2004. Preprint.
Goodman, J. & Xu, G., 1994. *Astrophys. J.*, **432**, 213.
Hawley, J. F. & Balbus, S. A., 1991. *Astrophys. J.*, **376**, 223.
Hawley, J. F. & Balbus, S. A., 1992. *Astrophys. J.*, **400**, 595.
Hawley, J. F., Gammie, C. F. & Balbus, S. A., 1995. *Astrophys. J.*, **440**, 742.
Julien, K. & Knobloch, E., 1997. *Phys. Fluids*, **9**, 1906.
Julien, K. & Knobloch, E., 1998. *J. Fluid Mech.*, **360**, 141.
Julien, K. & Knobloch, E., 1999. *Phys. Fluids*, **11**, 1469.
Julien, K., Knobloch, E. & Tobias, S., 1999. *Physica D*, **128**, 105.
Julien, K., Knobloch, E. & Tobias, S., 2000. *J. Fluid Mech.*, **410**, 285.
Julien, K., Knobloch, E. & Werne, J., 1998. *Theoret. Comput. Fluid Dynamics*, **11**, 251.
Julien, K., Sprague, M., Knobloch, E. & Werne J., 2005. Preprint.
Kawahara, G. & Kida, S., 2001. *J. Fluid Mech.*, **449**, 291.
Kersalé, E., Hughes, D. W., Ogilvie, G. I., Tobias, S. M. & Weiss, N. O. 2004. *Astrophys. J.*, **602**, 892.
Knobloch, E., 1992. *Mon. Not. R. astr. Soc.*, **255**, 25p.
Knobloch, E., 1996. *Phys. Fluids*, **8**, 1446.
Knobloch, E. & Spruit, H. C., 1986. *Astron. Astrophys.*, **166**, 359.
Matthews, P. C., 1999. *J. Fluid Mech.*, **387**, 397.
Papaloizou, J. C. B. & Pringle, J. E., 1984. *Mon. Not. R. astr. Soc.*, **208**, 721.
Rózyczka, M. & Spruit, H. C., 1993. *Astron. Astrophys.*, **417**, 677.
Ryu, D., & Goodman, J., 1992. *Astrophys. J.*, **388**, 438.
Shakura, N. I., & Sunyaev, R. A., 1973. *Astron. Astrophys.*, **24**, 337.
Stone, J. M., & Balbus, S. A., 1996. *Astrophys. J.*, **464**, 364.
Velikhov, E. P., 1959. *Sov. Phys. JETP*, **36**, 995.

This paper has been typeset from a TEX/ LATEX file prepared by the author.